Annual Scientific Report

on

INFRARED SIGNATURE MASKING BY AIR PLASMA RADIATION

Grant No. NAG 2-1079

Prepared for

NATIONAL AERONAUTICS AND SPACE ADMINISTRATION

For the Period

June 1, 1996 to March 31, 1997

Submitted by

C. H. Kruger, Principal Investigator
C. O. Laux, Associate Investigator

HIGH TEMPERATURE GASDYNAMICS LABORATORY
Mechanical Engineering Department
Stanford University

CONTENTS

1. Introduction

This report describes progress on the first year of a research program on the infrared radiation of air plasmas conducted in the High Temperature Gasdynamics Laboratory at Stanford University. This research is supported by a grant from the National Aeronautics and Space Administration (NAG 2-1079) and is currently under the direction of Professor Charles H. Kruger, with Dr. Stephen R. Langhoff from NASA-Ames as technical monitor. One Ph.D. candidate is currently involved in this program.

This program is intended to investigate the masking of infrared signatures by the air plasma formed behind the bow shock of high velocity missiles. In a previous program (Grant NAG 2-910), spectral measurements were made of the radiation emitted between 1 and 5.5 μm by an atmospheric pressure air plasma in chemical and thermal equilibrium at a temperature of approximately 7,900 K. These measurements revealed the presence of an intense radiation continuum between 3 and 5 μm, a critical spectral range for the detection of infrared missile signatures. The measured continuum was found to be underpredicted by the baseline NEQAIR code, as can be seen in Fig. 1 where the simulated continuum only accounts for approximately 25% of the measured continuum. The reasons for this discrepancy are examined in Section 2 of this report. Section 3 presents measurements of the infrared radiation emitted by air plasmas at a significantly lower temperature (~3000 K). The two temperature regimes investigated in this and the previous program represent extreme cases that provide insight into the phenomena encountered in the nonequilibrium bow shock of hypervelocity missile interceptors.

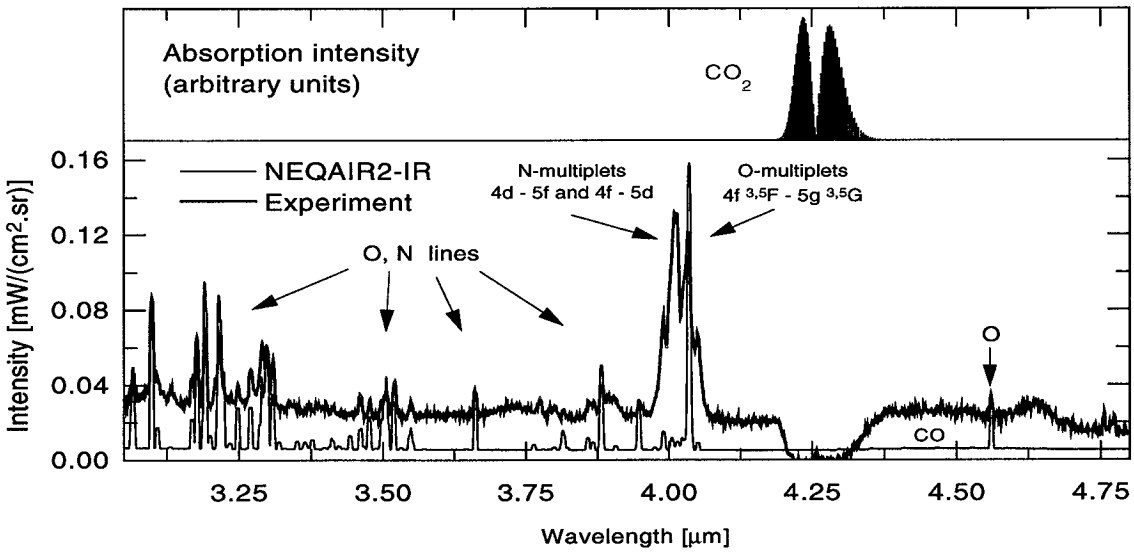

Figure 1. Bottom: Measurements and simulations[1] between 3.0 and 4.8 μm. Top: Absorption spectrum of CO_2 at 273 K.

2. Continuum Radiation of Air Plasmas

2.1. Introduction

Continuum radiation results from the interaction between two particles of which at least one is charged. The interaction produces radiation only if the two particles have different charges in the dipole approximation (quadrupole emission is usually negligible). Therefore e–e, e–A^-, A^-–A^-, A^+–A^+ interactions (where A is any neutral species) do not radiate. It is generally sufficient to consider the interaction between electrons and heavy particles because the deviation, and hence the emission, of ions is much smaller (~1/1000) than that of electrons owing to their greater mass. The particles interacting with electrons can be considered fixed before impact since the speed of electrons is usually much higher (~100 times) than that of heavy species. Furthermore, because of the large mass difference, heavy species can be considered immobile during the entire collision.

Two main types of interaction exist:

- **Absorption/emission of electrons: free-bound radiation**

Free-bound radiation occurs when an electron is absorbed by an ion or neutral. Bound-free radiation is the reverse process and is accompanied by the emission of electrons. This is calculated by NEQAIR in subroutine BFCONT.

- **Deviation of electron trajectories: free-free radiation**

Radiation is emitted when an electron is accelerated, namely when its trajectory is curved by another particle. This radiation is called "free-free" radiation, or Bremsstrahlung, and accompanies the scattering of electrons. Free-free radiation is computed by NEQAIR in subroutine FFCONT.

In turn, these interactions can be subdivided into four types:

- free-free with ions: $e+A^+ \rightarrow e+A^++h\nu$
- free-free with neutrals: $e+A \rightarrow e+A+h\nu$
- free-bound with ions: $e+A^+ \rightarrow A+h\nu$
- free-bound with neutrals: $e+A \rightarrow A^-+h\nu$

Because the continuum is essentially structureless, it is difficult to separate the contributions of the various species and types of continua. Thus discrepancies often exist between measured and calculated continua. In this section, we describe various forms of continuum radiation, including the free-free and free-bound of neutral and ions, then present an analysis of the causes for the discrepancy between modeled and measured continuum. Preliminary efforts to enhance the free-free continuum modeling of NEQAIR are also discussed.

2.2. Free-free with ions:

2.2.1. Background

The free-free electron-ion interaction takes place in the wide-range coulomb field of the ions, and therefore the strength of the interaction is roughly the same for the ion of any atom or molecule. For the temperature range of the present study (T < 8000 K), only positive (singly charged) ions need to be considered since their concentration is always much greater (~100 times) than that of negative ions (see Fig. 3). As can be seen from Fig. 3, the dominant ions are: NO^+ below 6000 K, N^+, O^+, NO^+ between 6000 and 9000 K, and N^+, O^+ above 9000 K.

The free-free interaction is theoretically well known because it results from a wide range field which allows quasi-classical-hydrogenic calculations to a good approximation. The equation describing this free-free radiation was derived by Kramers[2] and is called Kramers equation (the free-free with ion is also called Kramers radiation). It gives the absorption coefficient α_i for species i, stimulated emission not included:

$$\alpha_i = \frac{4}{3}\left(\frac{2\pi}{3kT_e m_e}\right)^{\frac{1}{2}} \frac{e^6}{(4\pi\varepsilon_0)^3 h m_e c \upsilon^3} Z^2 n_i n_e \qquad [m^{-1}]$$

$$= 3.68\times10^{-2}\frac{Z^2 n_i n_e}{\sqrt{T_e}\,\upsilon^3} \qquad [m^{-1}] \qquad (1)$$

where T_e is the electron temperature, n_i the density of species i [m^{-3}], Z the charge of the ion, and υ the frequency.

Several authors have proposed refinements to Kramers equation in the form of corrective factors determined from quantum mechanics:

<u>non-classical correction:</u>

In this case the RHS of Eqn. 1 is multiplied by a factor ξ, called the Biberman factor, which is the Maxwellian average of the so-called Gaunt factor.[3]

<u>non-hydrogenic correction</u>:

Peach[4-8] proposed to multiply the RHS of Eqn. 1 by a factor (1+D) that includes the g factor. This correction is the one applied in NEQAIR.

Because Kramers equation is a very good approximation, these factors are usually close to unity, as illustrated in Fig. 2 with the spectral correction factor (used in NEQAIR) for atomic nitrogen.

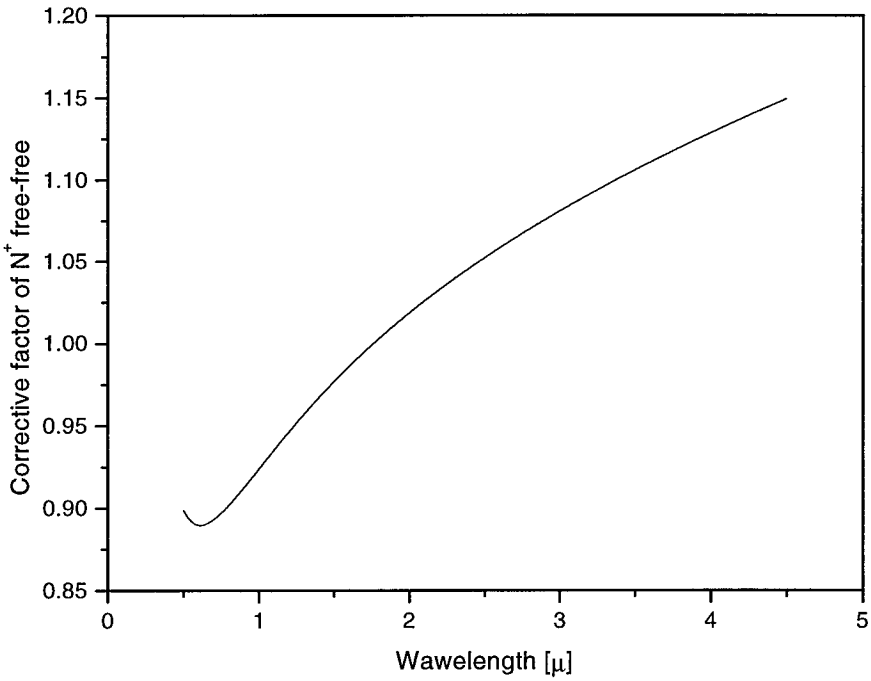

Figure 2. Correction factor for the free-free of N^+ in NEQAIR.

2.2.2. Changes to NEQAIR model of ion free-free

The study of subroutines FFCONT and BFCONT brought to light some inaccuracies that we have corrected as detailed below.

1) The NEQAIR routine used to compute the ion free-free is FFCONT. It calculates the correction factor for only two species, N^+ and O^+, because NEQAIR was initially intended for T>10000K where the dominant ions are N^+ and O^+ (see Fig. 3). However the dominant ion in the temperature range of interest here (T<8000K) is NO^+ and thus must be included in the calculations. The total free-free absorption coefficient from ions can be written as follows:

$$\alpha = \sum_{ions} A(T) n_i g_i = A(T) \sum_{ions} n_i g_i$$

where n_i is the density of ion i, g_i the correction factor for ion i, and (from Eqn. 1):

$$A(T) = 3.68 \times 10^{-2} \frac{Z^2 n_e}{\sqrt{T} \upsilon^3}.$$

In a first approximation we considered g_i=1 for all ions, which is probably a good approximation since free-free correction factors are close to unity. It follows, since the plasma is neutral:

$$\alpha = A(T) \sum_i n_i = A(T) n_e$$

Additional work is required to determine more accurate values for the correction factors of all ions. Nevertheless it can be seen from Table 1 that it is essential to model the free-free due to all ions. The correction has an appreciable effect on the values of the ion free-free continuum computed by NEQAIR for the experimental conditions[1] corresponding to Fig. 1.

Table 1. Free-free continuum computed by the baseline NEQAIR and the modified version taking into account all ions.

	Spectral radiance [mW/(cm^2-sr)] at 3.75 μm for our experimental conditions[1] (~8000 K)
Measurement	0.03
Baseline NEQAIR (N^+,O^+ free-free)	0.0058
NEQAIR (all ions free-free)	0.0083

At the temperatures of interest to the missile signature masking problem, the correction is even more important since O^+ and N^+ are negligible. At 6000K, for instance, NO^+ produces over 200 times the radiation of these ions.

2) In NEQAIR, the emission coefficient E_λ is derived using the following relation:

$$E_\lambda = B_\lambda \, \alpha'_\lambda$$

where α'_λ is the "apparent" absorption coefficient (i.e. including stimulated emission) and B_λ the Planck function. Currently, however, the subroutine FFCONT produces the "true" absorption coefficient (i.e. ignoring stimulated emission) computed with Kramers equation (Zeldovich and Raizer,[9] p. 260).

We corrected this error by multiplying α_λ in FFCONT by $1-\exp(-h\nu/kT)$ to obtain α'_λ. This correction is not negligible since $h\nu/kT$ is of the order of 1 at our temperature and wavelength conditions. At 3.75 μm and for the conditions of Fig. 1, this correction results in the effective decrease of the computed continuum emission coefficient by a factor of 2.5 (Table 2).

The spectrum computed between 3-5 μm with these two corrections is shown in Fig. 5.

Table 2. Effect of stimulated emission on the spectral radiance in NEQAIR.

	Spectral radiance [mW/(cm^2-sr)] at 3.75 μm for our experimental conditions[1] (~8000K)
Measurement	0.03
NEQAIR accounting for all ions	0.0083
NEQAIR accounting for all ions and stimulated emission	0.0033

2.3. Free-free with neutrals

2.3.1. Background

The neutral free-free is due to the interaction of electrons with the electronic orbitals of atoms and molecules. The nature of this interaction is very different from the ion free-free, as mentioned by Geltman[10] (p. 601) and John and Williams[11] (p. 169), because unlike electron-ion collisions, the electron-neutral interaction occurs at very short range (atomic orbitals).

In air plasmas, the major species interacting with electrons are [N_2, O_2] below 2000 K, [N_2, O, O_2, NO] between 2000 and 5000 K, and [N, O, N_2] for temperatures above 5000 K. Molecules are expected to have a larger free-free emission cross-section than atoms since the interaction highly depends on the scattering efficiency.

The neutral free-free absorption cross-section is directly related to the elastic electron scattering cross-section,[12,13] or to the momentum transfer cross-section.[9,14] The relation proposed by Cabannes and Chapelle[12,13] was recently used in computations of the neutral free-free by Menart et al.[15] and by Wilbers et al.[16] The electron scattering cross-sections of neutrals are generally one to two orders of magnitude smaller than those of ions. As a result, in highly ionized gases (T> 10,000 K) only the ion free-free is of importance. Below 8000 K, however, it can be seen in Fig. 3 that the concentration of neutrals is at least 3 orders of magnitude larger than ions, and therefore their free-free radiation cannot be neglected, contrary to what was done in certain references.[3] Experimental results reported by Taylor[17] (see Fig. 4) support the same. It is thus important to have an accurate description of this continuum.

Neutral free-free has been the object of theoretical and experimental work during the 1960's, in the context of the space program, and theoretical work in recent years. As will be seen below, however, there does not appear to be a consensus on the treatment of electron-neutral interactions.

The models presented in the literature use various approximations: for example, multichannel theory,[11] electron scattering or momentum transfer cross-sections,[12,14,18] atomic potential,[10] quantum defect,[4,19] and polarization of the target.[20]

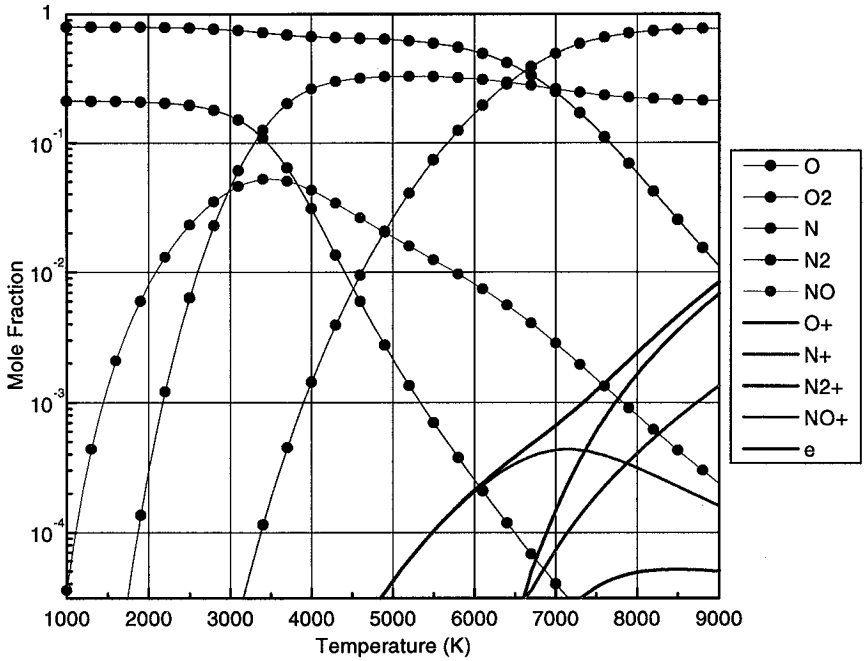

Figure 3. Mole fractions of major species in pure air between 800 and 9000K. At all temperatures, the mole fractions of negative ions remain below 10^{-6}.

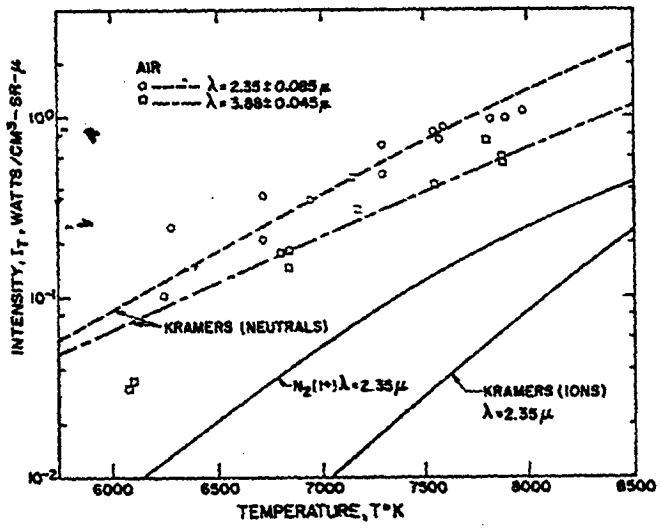

Figure 4. Experimental results[17] showing the relative importance of ion and neutral continua.

Few measurements have been made of the neutral free-free continuum in the temperature and wavelength range of interest for the present work (T<8000K, 1<λ<5μm). With regards to electron scattering cross-sections, accurate measurements[21-23] and calculations[22,24,25] have been made for NO, N_2, and O_2. However, there are few measurements and theoretical calculations[26,27] for O, and only calculations for N.[24,26]

Moreover, the authors use theoretical expressions to separate the contributions of individual species to the neutral continuum, which leads to questionable results as these theoretical expressions may not be accurate. The value of the total neutral free-free radiation is more reliable in these experiments since it is simply obtained by subtracting the relatively well-known ion free-free (Kramers radiation) from the measured continuum.

The evaluation of the intensity of the total continuum itself is further hindered by the presence of superimposed molecular bands. As can be seen in Fig. 5 (taken from Ref. [1]), the presence of molecular bands between 3 and 5.5 μm in the measured spectrum may partly contribute to the continuum. The intensity of this molecular emission of unknown origin can be estimated from the drop indicated at 4.8 μm where the real level of the continuum might appear because of the absence of molecular bands.

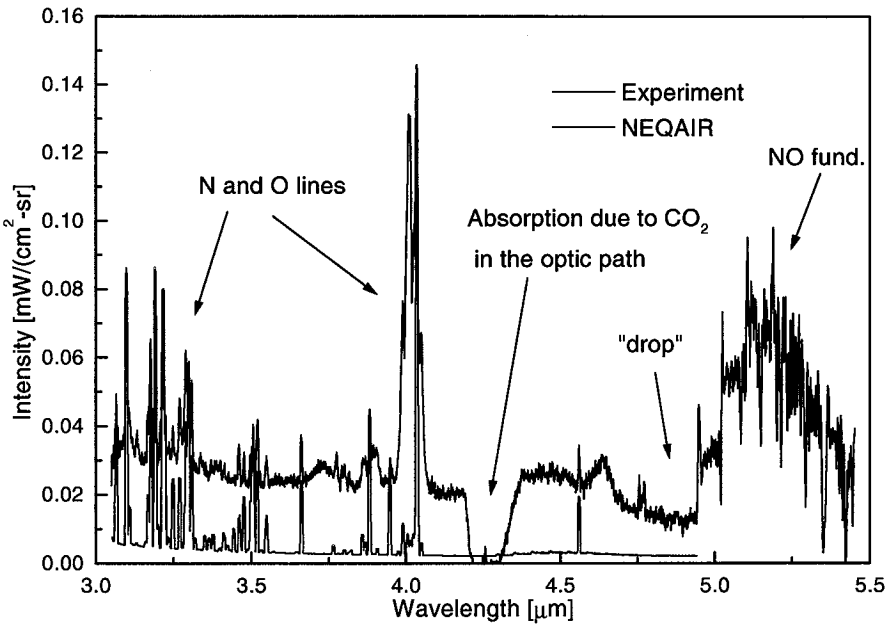

Figure 5. Experimental[1] and computed IR radiation of high temperature air. Continuum computations are limited to the ion free-free.

A review of the cross-sections reported in the literature indicates that large discrepancies exist between calculations and measurements of the free-free continuum. As an illustration, selected values are given in Tables 3-5 of the free-free absorption cross-section Q_{a_i} defined by:

$$\alpha_i = n_e n_{a_i} Q_{a_i} \qquad (Q_{a_i} \text{ in } cm^5)$$

where α_i [cm^{-1}] is the absorption coefficient without stimulated emission and n_i [cm^{-3}] the density of species i.

Table 3. Free-free absorption cross-sections [10^{-38} cm^5]. Sample theoretical and experimental values for Ar and Ne.

Species	T(K)	λ (μm)	Theory Geltman[10]	Experiment Taylor and Caledonia[28,29]	Experiment Kung and Chang[30]
Ar	9700	3.1	2.5	10	7.5
Ne	12600	3.1	1.8	1.9	6.9
		9.85	52		78

Table 4. Free-free absorption cross-sections [10^{-38} cm^5] for O at ~10,000 K.

λ (μm)	Theory Chung and Lin[20] 10,000 K	Theory Geltman[10] 10,000 K	Theory John and Williams[11] 9700 K	Experiment Taylor and Caledonia[28,29]	Experiment Kung and Chang[30]
2	0.972	0.713	0. 96		
3.1		2.25 (9700 K)		7.6 (9700 K)	7.8 (9700 K)
3.5	4.63		4.67		
5	12.8	8.97	13.1		
9.85		65.2 (9700 K)			300 (9700 K)
10	96.6	66.8			

Table 5. Calculated free-free absorption cross-sections [10^{-38} cm^5] for O at ~5000 K

λ(μ)	Theory Chung and Lin[20] 5000 K	Theory John and Williams[11] 5040 K
1.14	0.12	0.109
1.52	0.25	0.228
2.28	0.73	0.66
4.56	4.9	4.38

As can be seen from Tables 3-5, discrepancies between computations and measurements often exceed a factor 4. Furthermore, the various models predict different dependence on the temperature for the atomic species. In the case of atomic oxygen for example, the model of Kivel[14] (see Table 8) predicts that the free-free continuum is independent of temperature, contrary to the experimental and theoretical results listed in Tables 4 and 5.

Table 6-7. Temperature and wavelength dependence of semi-empirical free-free cross-sections for O_2 and N_2 (Kivel[18]) [10^{-38} cm^5].

O_2

λ(μm)	6000K	9000K	12,000K
1.2	0.09	0.167	0.26
2.4	0.69	1.3	2.03
4.8	5.33	10.1	16

N_2

λ(μm)	6000K	9000K	12,000K
1.2	0.173	0.36	0.587
2.4	1.28	2.69	4.42
4.8	9.83	20.7	34.3

Table 8-9. Temperature and wavelength dependence of theoretical free-free cross-sections for O and N (Kivel[14,18]) [10^{-38} cm^5].

O

λ(μm)	6000K	12,000K
1.2	0.05	0.05
2.4	0.4	0.4
4.8	3.15	3.15

N

λ(μm)	6000K	12,000K
1.2	0.18	0.18
2.4	1.1	1.1
4.8	8	8

Much care should be taken with these results since no physical description of the neutral free-free is used to extract these data from experiment, as we already mentioned. For example Taylor[17] and Morris[31] use Kramers equation (Eqn. 1) for electron-neutral interaction whereas it was derived for electron-ion free-free. They use a Z^2 factor in the equation as a parameter, an "effective charge" determined experimentally, to allow comparison with the electron-ion free-free radiation where Z=1. There is however no theoretical justification for the use of the Z^2 factor (Taylor and Caledonia[28] p. 664). Moreover, while Morris[31] shows over a wide spectral range (0.097 - 0.7 μm) that Z^2 depends on the frequency (Fig. 6), Taylor (albeit operating in a shorter spectral range) finds Z^2 to remain approximately constant (Fig. 7).

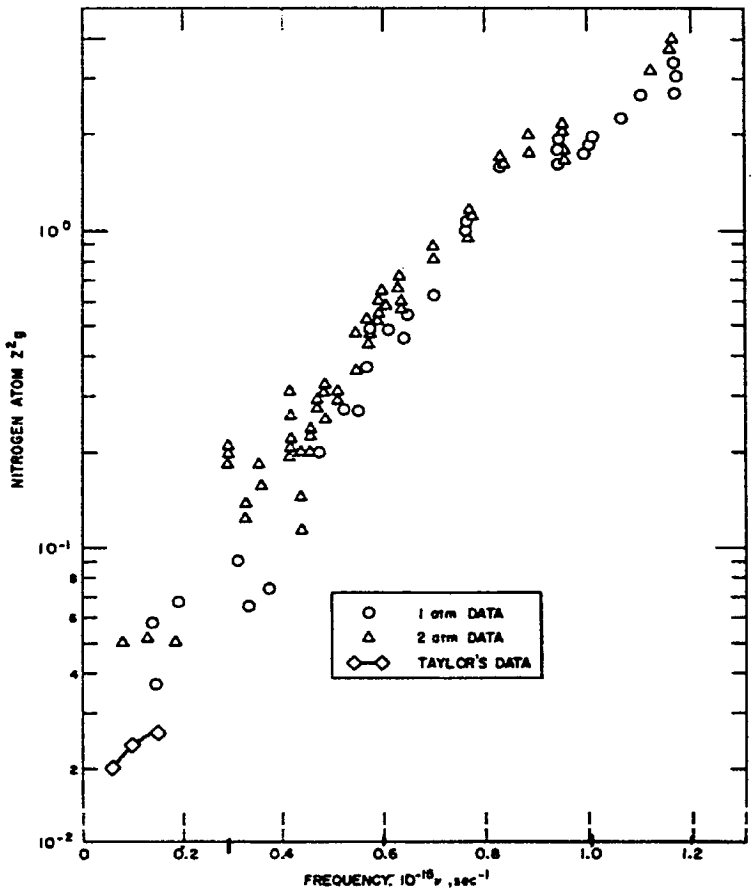

Figure 6. Effective charge factor Z^2 for atomic nitrogen (Morris[31] and Taylor[17]).

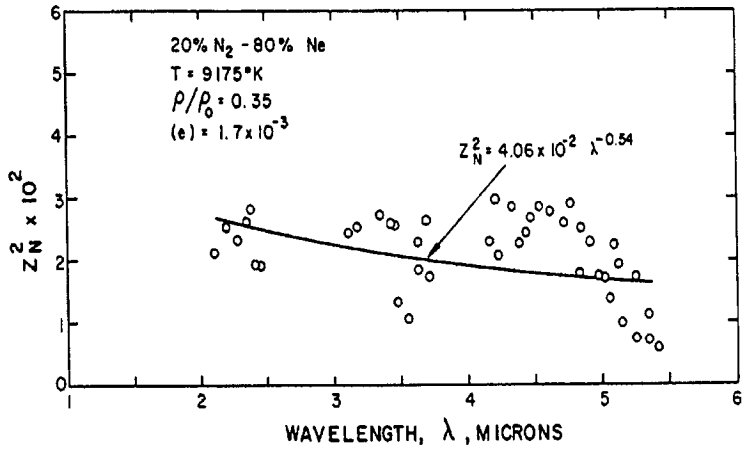

Figure 7. Effective charge factor Z^2 for atomic nitrogen (Taylor and Caledonia[29]).

2.3.2. *NEQAIR96 model*

Although the free-free continuum of neutrals was not modeled in the original NEQAIR code,[32] a model for neutral free-free was incorporated in the recent version NEQAIR96[33] using equations derived by Peach.[5-8] We suspect however that Peach's equations are not applicable for neutrals for the following reasons.

Peach[4] derived his correction factor explicitly for ions. Then[5-8] this correction factor was applied to the free-free cross-sections of Menzel and Pekeris[34] which are also explicitly for ions (Menzel and Pekeris[34] refer to Nedelsky[35] for electron-neutral interactions). Owing to the very different nature of the electron-neutral and electron-ion interactions, it is unlikely that Peach's results apply for neutrals. We are currently investigating other models[12,14,18,36] and completing a literature search for additional data regarding the neutral free-free continuum.

2.3.3. *Estimate of the importance of the neutral free-free*

In this section, we investigate the importance of the neutral free-free continuum in the temperature range of interest to the BMDO. Note again that there is no model of the neutral free-free in the original NEQAIR code. The Kivel cross-sections[18] are used for consistency as they are given for the 3 species of interest here, i.e. N, O, and N_2. The comparisons presented below are made at 4.8 μm.

As a first approximation, the plasma is modeled as a 2 cm slab of uniform temperature at 7800 K. This approximation is reasonable since the bulk of the radiation comes from the central part of the plasma which is at a temperature of approximately 7800 K (see Fig. 8). We will compare for convenience E_{exp} [W/(cm^2-sr)]/2cm and E_{calc} [W/(cm^3-sr)]. The neutral free-free absorption coefficient without stimulated emission is defined as

$$\alpha_i = n_e n_{a_i} Q_{a_i},$$

where Q_{ai}, n_{ai}, and α_i have dimensions of m^5, m^{-3} and m^{-1}, respectively. The cross-sections are obtained from Kivel.[14,18] We multiply α_i by $(1-\exp(-h\nu/kT))$ to account for stimulated emission, and by the Planck function:

$$B_\lambda = \frac{2hc^2}{\lambda^5}\left(e^{-\frac{h\nu}{kT}} - 1\right)^{-1}$$

to obtain the emission coefficient. The neutral free-free emission coefficient is then defined by the following equation:

$$E_{\lambda,neutral} = \frac{2hc^2}{\lambda^5} e^{-\frac{h\nu}{kT}} \alpha_i \quad \text{[W/(m}^4\text{-sr)]}$$

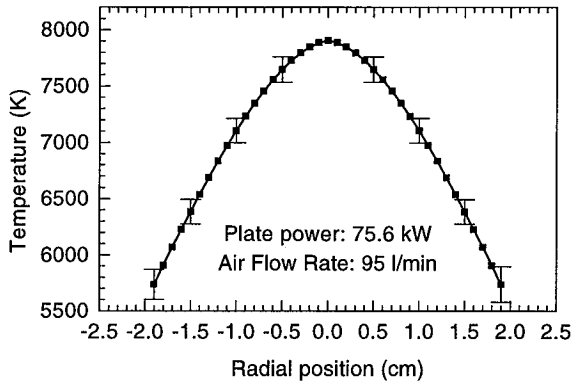

Figure 8. Temperature profile of the plume in experiment of Fig. 1.

As the experimental spectrum is convolved with the slit function of the monochromator, we also have to convolve $E_{\lambda,neutral}$ with the same slit function, which has an equivalent width of 0.0065μm. The continuum varies slowly over the equivalent slit width and thus the convolution is simply a multiplication. We finally have:

$$E_{neutrals} = 6.5\times10^{-10} n_e n_a Q_a \frac{2hc^2}{\lambda^5} e^{-\frac{h\upsilon}{kT}} \left[\mathrm{W/(m^3 - sr)}\right] \quad (2)$$

In turn, the free-free with ions can be determined from Kramers equation (Eqn. 1) with $n_i=n_e$. The resulting value of α does not take into account stimulated emission, as mentioned in section 2.2.2, so we apply the same correction as for the neutral free-free. Finally we have:

$$E_{ions} = 6.5\times10^{-10} \frac{2hc^2}{\lambda^5} e^{-\frac{h\nu}{kT}} \times 3.68\times10^{-2} \frac{Z^2 n_e^{\,2}}{\nu^3\sqrt{T}} \left[\mathrm{W/(m^3 - sr)}\right] \quad (3)$$

The data used for the present calculations are given in Table 10, and the resulting radiative coefficients are summarized in Table 11. In Table 11, E_i is the free-free emission coefficient and α_i the free-free absorption coefficient of species i.

Table 10. Air composition and neutral free-free cross-sections at T=7800 K and λ=4.8 μm (from Kivel[14,18]).

Species	Air Composition T=7800 K, P=1atm n_a [cm^{-3}]	Free-free Cross-section (Kivel[14,18]) Q_a [cm^5]	Cross-section per unit volume n_aQ_a [cm^2]
e	1.8×10^{15}		
O	20.3×10^{16}	3.15×10^{-38}	6.4×10^{-21}
N_2	7.23×10^{16}	16.6×10^{-38}	12×10^{-21}
N	62.5×10^{16}	8×10^{-38}	50×10^{-21}

The cross-section per unit volume, n_aQ_a, represents the contribution of each species to the total absorption. We notice that N is the dominant neutral for free-free radiation at 7800 K.

Table 11. Calculated radiative coefficients for neutral and ions compared to measured continuum.

	E_i [10^{-7} W/(cm^{3}sr)]	α_i [10^{-5} cm^{-1}]
O (Eqn. 2)	2.2	1.15
N_2 (Eqn. 2)	4.2	2.16
N (Eqn. 2)	17	9
Total neutral free-free	23.4	12.31
Total ions free-free (Eqn. 3)	11.4	
Total free-free (neutral + ions)	**34.8**	
Measured continuum at 4.8μm	**60**	

Note: The total ion free-free computed with NEQAIR using the full measured temperature profile of Fig. 8 is equal to E_{ions}/2cm=9.5×10^{-7} W/(cm^3-sr). This value is very close to the value of 11.4×10^{-7} W/(cm^3-sr) that we obtained with the assumption of a 2 cm plasma of uniform temperature 7800 K.

Thus, the total estimated free-free emission 34.8×10^{-7} [W/(cm^{3}sr)] represents approximately half the measured continuum E_{exp}/2cm=60×10^{-7} [W/(cm^{3}sr)]. The neutral free-free alone represents more than a third of the measured continuum. Uncertainties certainly remain (for instance, Kivel[14,18] gives Q=4×10^{-39} cm^5 for atomic oxygen whereas John and Williams[11] give Q=10^{-38} cm^5), but nevertheless the neutral free-free appears as a very important emission process in the infrared.

2.4. Free-bound with ions

The ion free-bound continuum is described by the following process

$$A^+ + e \leftrightarrow A^* + h\upsilon,$$

where A^* represents an electronic state of the neutral species A. The theory is well known for this interaction, and the photoionization cross-sections required for the determination of the emission coefficient have been calculated or measured for many atoms.

The model used in NEQAIR is based on the free-bound Kramers equation with the correction of Peach. As for free-free radiation we corrected the emission coefficient for stimulated emission.

However there are currently two limitations in the NEQAIR model. First, as for the ion free-free, only N^+ and O^+ are taken into account. As already discussed, additional ions must be considered at temperatures below 9000 K. Second, the bound-free radiation stops at 1.4 microns which means that there is a cut-off for the higher energy levels of the atoms. Bound-free absorption from high lying atomic and molecular levels should therefore be considered. We are currently investigating methods to remove these limitations.

2.5. Free-bound with neutrals

The neutral free-bound continuum, or attachment, is described by the following process

$$A + e \leftrightarrow A^- + h\upsilon$$

This process is the reverse of the so-called photo-detachment. It is particularly important for electronegative species such as O_2 and O. As several references[31,37-39] mention the importance of the resulting radiation, further work is required to incorporate this continuum into NEQAIR2-IR.

3. Infrared Radiation Measurements in Air at ~3000 K.

Infrared radiation measurements were made at temperatures close to 3000 K in order to provide additional validation data for the radiation code NEQAIR2-IR. These experiments complement the previous set of measurements at ~8000 K, and bracket the temperature range of interest to the hypervelocity missile bow-shock conditions.

The 3000 K air plasma was generated by cooling an air plasma initially at ~7500 K through a water-cooled brass test-section of length 60 cm, as shown in Fig. 9. The initial 7500 K plasma was produced with a 50 kW TAFA model 66 RF induction plasma torch, powered by a LEPEL model T-50-3 power supply operating at a frequency of 4 MHz. The plasma torch facility and the set-up for experimental measurements are described in Ref. [1]. The infrared spectrum emitted across the plasma diameter was recorded between 3 and 5.5 μm using a scanning monochromator (SPEX Model 750M) fitted with a 300 gr/mm grating blazed at 4 μm. A long pass filter ($\lambda > 3$ μm) was inserted in the optical path to reject second order radiation from the region $\lambda < 3$ μm. The entrance and exit slits of the monochromator were set at 0.75 and 2.8 mm, respectively, thus yielding a trapezoidal slit function of base 140 Å and top 80 Å at 3 μm (As discussed in Ref. 1, the linear dispersion varies with wavelength. The correction factor determined in Ref. 1 was applied to the analysis of the present results). The measured spectrum was corrected for the spectral response of the detection system and calibrated in intensity using a tungsten lamp (Optronics Model 550) with calibration traceable to NIST standards. The accuracy of the measured spectral intensity is estimated to be better than 10% over the whole spectral range.

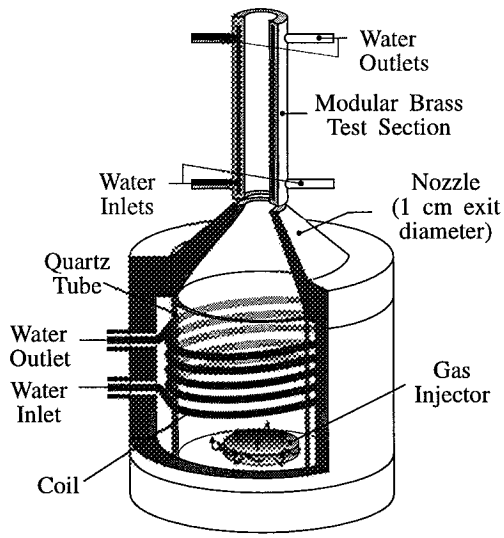

Figure 9. Plasma torch head and cooling test-section schematic.

The measured IR spectrum, shown in Fig. 10, exhibits two main spectral features: the fundamental NO (X-X) bands at ~5 μm, and the ν_3 band of CO_2 (antisymmetric stretch) at ~4.3 μm. Although the concentration of carbon dioxide was relatively small (approximately 330 parts per million, which is the natural CO_2 concentration in atmospheric air at room temperature), a large amount of radiation is emitted by the ν_3 band. CO_2 radiation may thus present a challenge for the detection of infrared signatures since under flight conditions an even larger amount of CO_2 may be present in the bow-shock as a result of carbon ablation from the interceptor's surface.

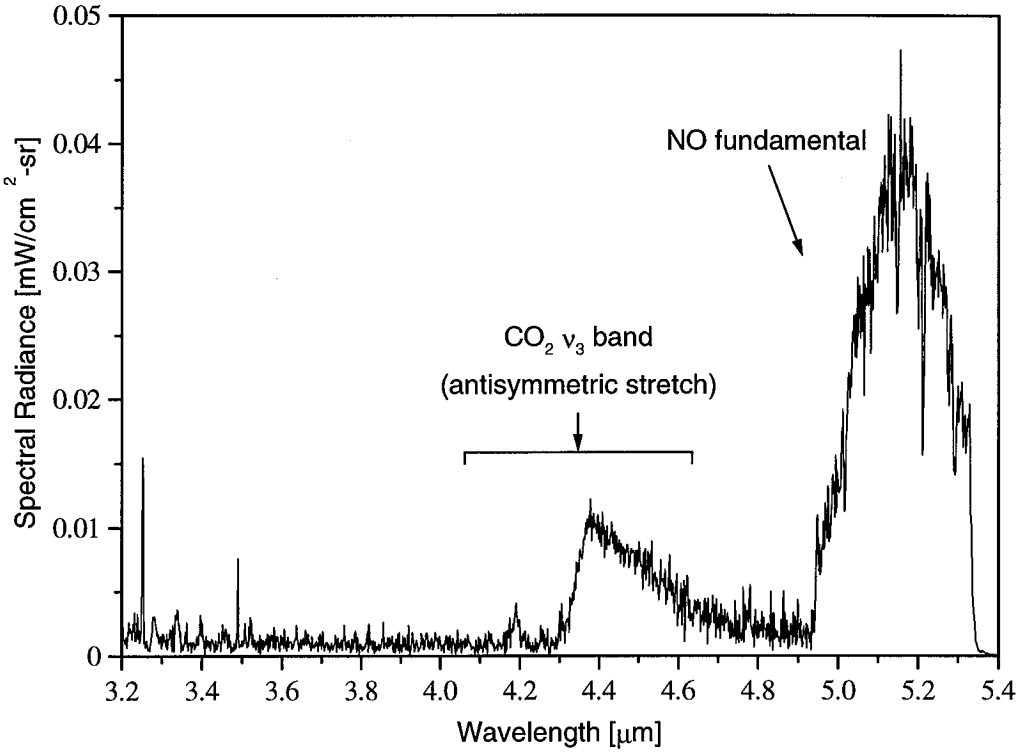

Figure 10. Measured IR emission spectrum for the 3000 K plasma.

For modeling purposes, the thermodynamic state of the plasma must be determined. As mentioned in Ref. [1], one important aspect of the present studies is that the air plasmas generated with the torch are close to Local Thermodynamic Equilibrium (LTE). The main benefit of using LTE plasmas is that the quantities needed to model their radiation (species concentrations, excited state distributions) can be fully determined, using equilibrium relations, with knowledge of only two parameters, the pressure (1 atm. here) and the temperature. In this case, the temperature profile (shown in Fig. 11) was measured from the Abel-inverted intensity of the NO fundamental (1-0) band head at 4.95 μm.

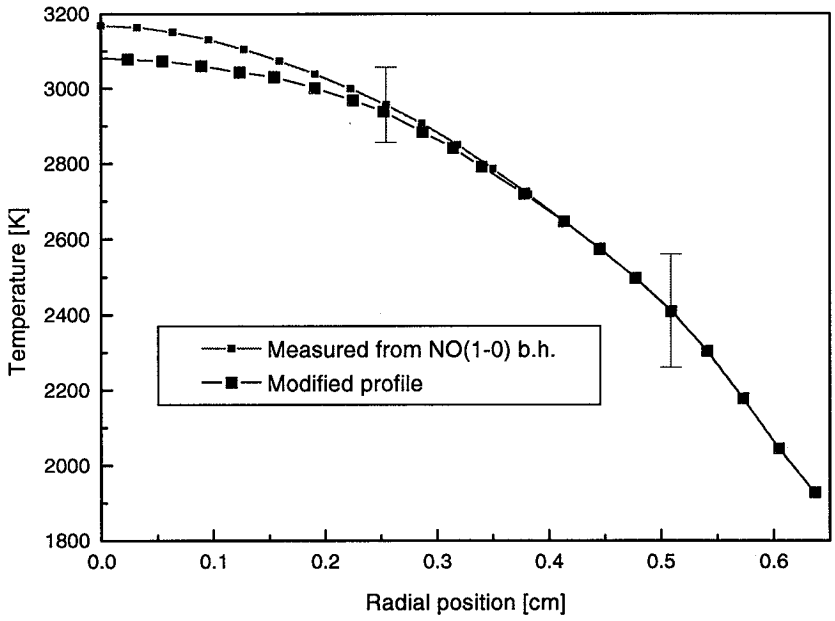

Figure 11. Measured (from the NO (1-0) band-head) and modified temperature profiles in the plasma.

In order to confirm the existence of LTE conditions in the plasma, additional measurements were made of the radiation emitted in the UV between 200 and 400 nm. For these measurements, the slit function is well approximated by a trapezoid of base 13.2 Å and top 4.4 Å. These measurements were then compared with LTE predictions of the NEQAIR2 code.[40] For these simulations, all necessary concentrations where determined from equilibrium relations using the temperature profile measured from the NO (1-0) band head. As can be seen in Fig. 12, the NEQAIR2 spectrum based on this profile overpredicts the measurements by approximately 50%. However, the intensities of the electronic transitions of importance in the 200-400 nm spectral range (NO Gamma (A→X), NO beta (B→X), and O_2 Schumann-Runge (B→X)) are very sensitive to the temperature in the central part of the plasma, and therefore a small error in the measured temperature there could be responsible for the discrepancy. Indeed, it was possible to reproduce the measured spectrum with the slightly altered temperature profile shown in Fig. 11. This modified profile was obtained by lowering the temperature in the central plasma region by ~100 K, a small change that is within the estimated uncertainty of the measured temperature. Note that the uncertainty of the temperature profile measured from the NO (1-0) band head is largest in the central part of the plasma. Therefore the temperature correction appears reasonable and justified. The NEQAIR2 spectrum computed with this modified profile, shown in Fig. 13, is in excellent agreement with the measurements, and thus supports the assumption of LTE in the plasma.

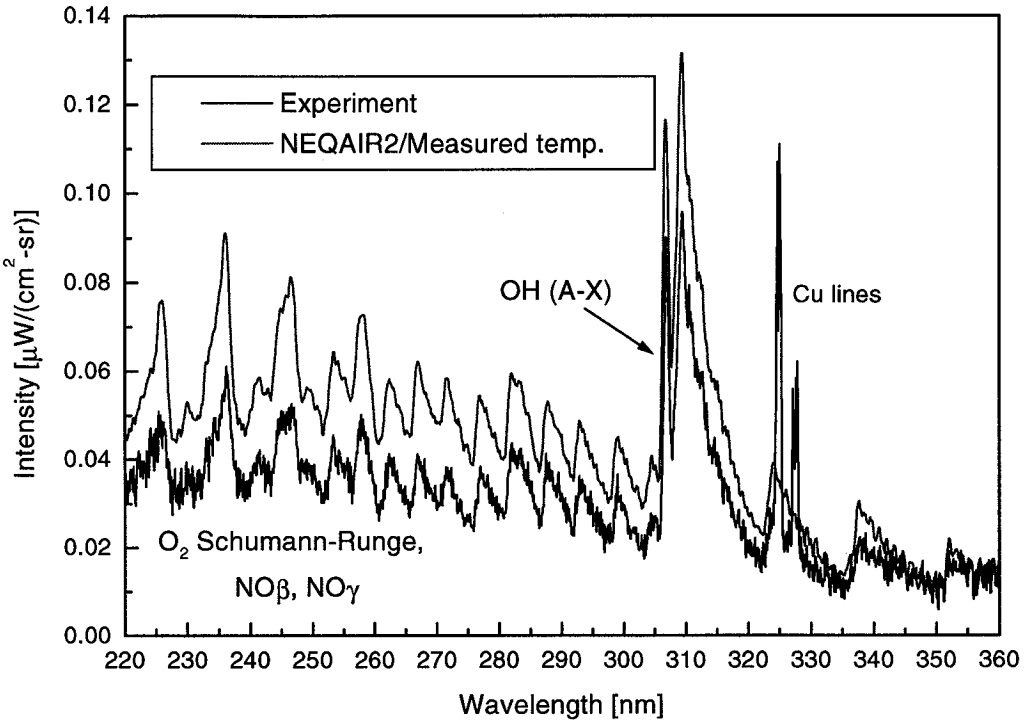

Figure 12. UV spectrum computed with NEQAIR using the measured temperature profile, and comparison with the experimental spectrum.

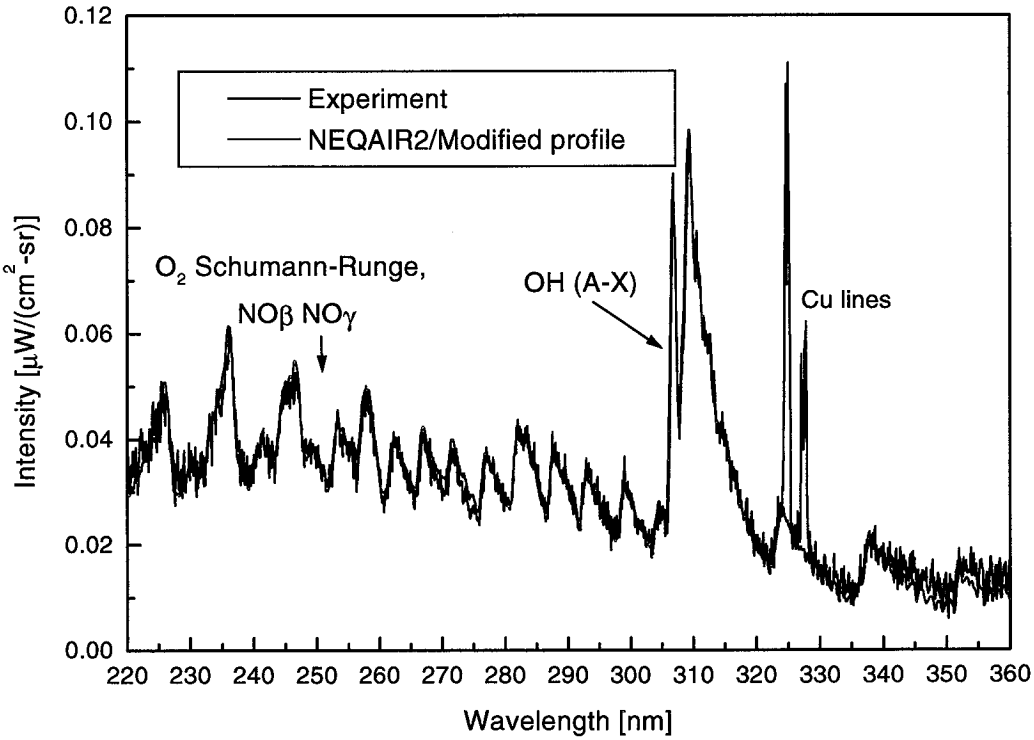

Figure 13. UV spectrum computed with NEQAIR2 using the modified temperature profile, and comparison with the experimental spectrum.

The air injected in the plasma torch was produced by compressing atmospheric air and therefore contained about 330 ppm of CO_2 and an undetermined amount of water vapor. By matching the absolute intensity of the measured and predicted A→X band of OH at ~307 nm, we determined the concentration of OH in the plasma and thus the mole fraction of atomic hydrogen. We concluded that the mole fraction of H_2O in the atmospheric pressure, 300 K air injected in the torch was approximately 3.8×10^{-4}. It is clear from the measured emission spectrum that neither water (nor OH) bands emit significantly in the infrared under our conditions.

Comparisons Model-Experiment:

In this section, we present comparisons between the measured infrared spectrum and the predictions of two spectral codes. Particular attention is paid to the dominant emitters, namely the fundamental vibrational bands of NO, and the ν_3 band of CO_2.

Figure 14 shows a comparison of results for the NO fundamental bands. Details on the NO radiation model incorporated into NEQAIR2-IR are presented in an earlier reference.[1] As can be seen in Fig. 14, the predictions of the model are in excellent agreement with the measured spectrum. It should be noted again that both the measurements and computations are on absolute scales.

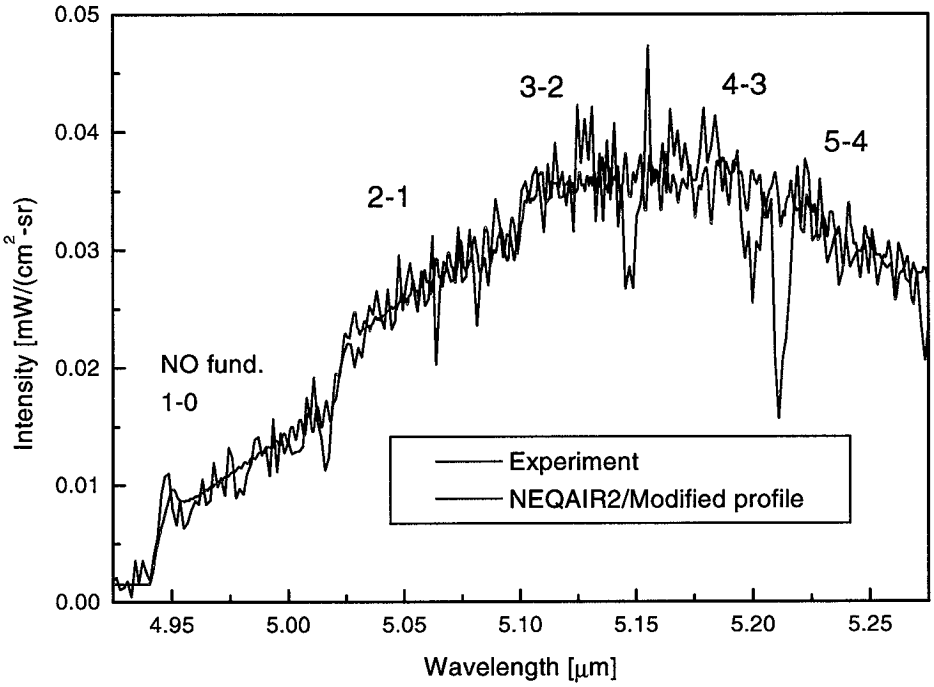

Figure 14. IR spectrum computed with NEQAIR2-IR using the modified temperature profile, and comparison with the experimental spectrum. The presence of water vapor in the optical path separating the plasma from the detector is responsible for the absorption features observed in particular at 5.02, 5.065, 5.08, 5.15, 5.20, and 5.22 μm.

Figure 15 compares the measured CO_2 ν_3 band spectrum with the predictions of the *correlated-k* model[41] based on the parameters of EM2C Laboratory of the Ecole Centrale Paris.[42,43] The *correlated-k* model is a narrow-band model in which the actual spectrum is replaced on each narrow band by the reordered spectrum, so that the spectral integration can be carried out using typically 10 points instead of several thousands. In the case of CO_2 IR radiation, this model affords radiative intensity predictions within a few percent accuracy.[43] The parameters used for the comparison shown in Fig. 15 are based on a 16-point gaussian quadrature and a spectral decomposition over intervals of width 25 cm^{-1}. The model also accounts for absorption by room air CO_2 over the optical path separating the plasma from the detector. This absorption is clearly responsible for near extinction in the range 4.2-4.3 μm of the emission from low-lying rotational levels of CO_2. The lines appearing at both edges of the absorbed region correspond to "hot" CO_2 rotational lines. Work is currently in progress to incorporate this model into NEQAIR2-IR.

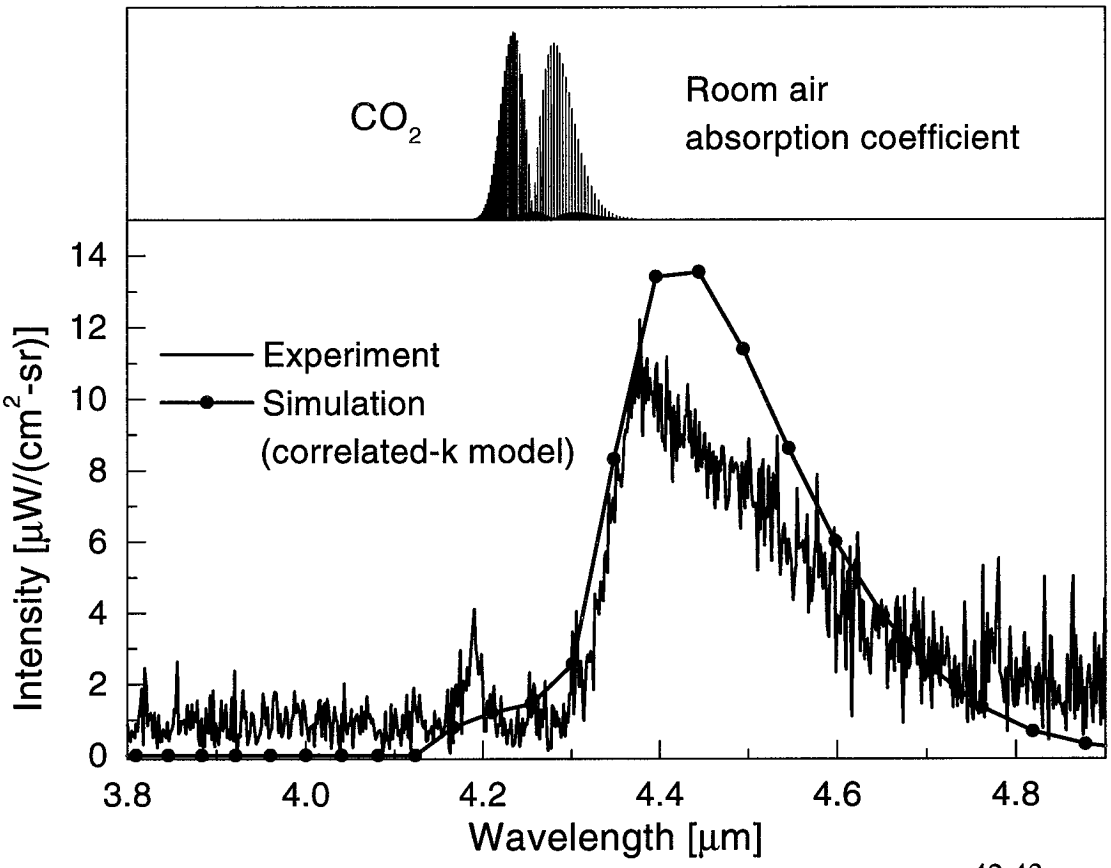

Figure 15. CO_2 spectrum computed with the *c-k* model parameters[42,43] of the EM2C Laboratory using the modified temperature profile, and comparison with the experimental spectrum.

4. Conclusion

Experimental benchmark spectra of the infrared emission of high-temperature air were measured at approximately 8000 K and 3000 K. These measurements were used to guide enhancements to the NEQAIR code, as already partly described in Ref. 1. Particular emphasis was placed in this report on the intense continuum observed between 3 and 5 μm, on the infrared bands of NO, and on the ν_3 band of CO_2 at 4.3 μm.

Several processes, namely the free-free and free-bound of both ions and neutrals, must be taken into account to describe the observed continuum.

The free-bound continuum corresponds to the radiative emission associated with the recombination of positive ions (or neutrals) into excited electronic states of the corresponding neutral (or negatively charged) species. The baseline NEQAIR code only models the free-bound (subroutine BFCONT) of two ions, N^+ and O^+. However, the dominant ion in air at temperatures below 8000 K is NO^+, and therefore the model must be modified to incorporate the NO^+ free-bound. Another limitation of the free-bound model of the baseline NEQAIR is that too few electronic levels are taken into account. As a result, free-bound radiation is only modeled at present for wavelengths shorter than ~1.4 micron. Finally, there is currently no model in NEQAIR for the free-bound recombination of neutral species (electron attachment/detachment).

The free-free continuum corresponds to the deviation of electron trajectories in the field of ions (ion free-free) or of the electronic orbitals of neutrals (neutral free-free). In the baseline NEQAIR, only the free-free continuum of ions is modeled (subroutine FFCONT). Yet, the preliminary analysis presented in this report indicates that the neutral free-free could represent as much as 40% of the total measured continuum at 8000 K, and an even larger fraction at lower temperatures.

Work is in progress to determine an optimal and accurate way to account for these various continuum processes and to incorporate them into NEQAIR2-IR. It should be noted that the ability to accurately model these processes is of great importance because the continuum radiation extends over the entire wavelength range of interest to the signature masking problem.

The spectroscopic model developed in our previous work[1] for the fundamental vibrational bands of NO is found to produce simulations in excellent agreement with the current measurements. Finally, the predictions of a low resolution (25 cm^{-1}) model[41-43] of the ν_3 band of CO_2 at 4.3 μm were compared with measurements and found to reproduce the observed CO_2 emission lines within 30%. Work is in progress to incorporate this CO_2 model into NEQAIR2-IR with higher spectral resolution.

5. Related Publications

Levin, D.A., Laux, C.O, and Kruger, C.H., "A General Model for the Spectral Calculation of OH Radiation in the Ultraviolet," submitted to JQSRT, March 1997.

Levin, D.A., Laux, C.O, and Kruger, C.H., "A General Model for the Spectral Calculation of OH Radiation in the Ultraviolet," AIAA 95-1990, 26th AIAA Plasmadynamics and Lasers Conference, San Diego, CA, June 19-22, 1995.

Laux, C.O., Gessman, R.J., Hilbert, B. and Kruger, C.H., "Experimental Study and Modeling of Infrared Air Plasma Radiation," AIAA 95-2124, 30th AIAA Thermophysics Conference, San Diego, CA, June 19-22, 1995.

6. Personnel

The following personnel contributed to this report:

Charles H. Kruger	Vice-Provost, Dean of Research and Graduate Policy, Professor, Dept. of Mechanical Engineering, Stanford University.
Christophe O. Laux	Research Associate, High Temperature Gasdynamics Laboratory, Department of Mechanical Engineering, Stanford University. (Ph.D. Mechanical Engineering, Stanford University, 1993).
Denis Packan	Graduate Research Assistant High Temperature Gasdynamics Laboratory, Department of Mechanical Engineering, Stanford University. (M.S. Engineering, Ecole Centrale Paris, 1996)
Richard J. Gessman	Graduate Research Assistant High Temperature Gasdynamics Laboratory, Department of Mechanical Engineering, Stanford University. (M.S. Engineering, University of Illinois at Urbana-Champaign, 1992)
Laurent C. Pierrot	Postdoctoral Fellow High Temperature Gasdynamics Laboratory, Department of Mechanical Engineering, Stanford University. (Ph.D. Mechanical Engineering, Ecole Centrale Paris, 1997)

7. References

[1]C.O. Laux, R.J. Gessman, B. Hilbert, and Kruger, C.H., "Experimental Study and Modeling of Infrared Air Plasma Radiation," 30th AIAA Thermophysics Conference **AIAA 95-2124** (1995).

[2]Kramers, Phil. Mag. **46**, 838 (1923).

[3]R. Lange and D. Schluter, "Free-free Emission Continuum of Weakly Non-Ideal Argon Plasmas," JQSRT **48** (2), 153-158 (1992).

[4]G. Peach, "A General Formula for the Calculation of Absorption Cross-Sections for Free-Free Transitions in the Field of Positive Ions," Monthly Notices of the Royal Astronomical Society **130**, 361-376 (1965).

[5]G. Peach, "Free-free Absorption Coefficients for Non-Hydrogenic Atoms," Memoirs of the Royal Astronomical Society **71**, 1-11 (1967).

[6]G. Peach, "A Revised General Formula for the Calculation of Atomic Photoionization Cross-Sections," Memoirs of the Royal Astronomical Society **71**, 13-27 (1967).

[7]G. Peach, "Total Continuous Absorption Coefficients for Complex Atoms," Memoirs of the Royal Astronomical Society **71**, 29-45 (1967).

[8]G. Peach, "Continuous Absorption Coefficients for Non-Hydrogenic Atoms," Memoirs of the Royal Astronomical Society **73**, 1-123 (1970).

[9]Y.B. Zeldovitch and Y.P. Raizer, *Physics of Shock Waves and High Temperature Hydrodynamic Phenomena* (Academic Press, New York, NY, 1966).

[10]S. Geltman, "Free-free Radiation in Electron-Neutral Atom Collisions," JQSRT **13**, 601-613 (1973).

[11]T.L. John and R.J. Williams, "Free-free Absorption by N^- and O^-," JQSRT **17**, 169-174 (1977).

[12]F. Cabannes and J.C. Chapelle, "Spectroscopic Plasma Diagnostics," in *Reactions under Plasma Conditions*, edited by M. Venugopalan (Wiley-Intersciences, New York, NY, 1971), Vol. 1, pp. 367-469.

[13]J. Chapelle and F. Cabannes, "Absorption et Emission du Rayonnement Continu Emis par un Jet de Chalumeau a Plasma d'Argon entre 30 et 30,000 cm^{-1}," JQSRT **9**, 889-919 (1969).

[14]B. Kivel, "Neutral Atom Bremsstrahlung," JQSRT **7**, 27-49 (1967).

[15]J. Menart, J. Heberlein, and E. Pfender, "Line-by-line Method of Calculating Emission Coefficients for Thermal Plasmas Consisting of Monatomic Species," JQSRT **56** (3), 377-398 (1996).

[16]A.T.M. Wilbers, Kroesen, G.M.W., Timmermans, C.J., Schram, D.C., "The Continuum Emission of an Arc Plasma," JQSRT **45** (1), 1-10 (1991).

[17]R.L. Taylor, "Continuum Infrared Radiation from High Temperature Air and Nitrogen," The Journal of Chemical Physics **39** (9), 2354-2360 (1963).

[18]B. Kivel, "Bremsstrahlung in Air," JQSRT **7**, 51-60 (1967).

[19]A. Burgess and M.J. Seaton, Monthly Notices of the Royal Astronomical Society **120**, 121 (1960).
[20]S. Chung and C.C. Lin, "Free-free Transitions in Collisions between Slow Electrons and Neutral Oxygen Atoms," Physical Review A **51** (2), 1221-1229 (1995).
[21]C. Szmytkowski and K. Maciag, "Absolute Electron Scattering Total Cross-Section Measurements for Noble Gas Atoms and Diatomic Molecules," Physica Scripta **54**, 271-280 (1996).
[22]M. Capitelli and R.S. Devoto, "Transport Coefficients of High Temperature Nitrogen," The Physics of Fluids **16** (11), 1835-1841 (1973).
[23]S. Trajmar, D.F. Register, and A. Chutjian, "Electron Scattering by Molecules. II. Experimental Methods and Data," Physics Reports **97** (5), 219-356 (1983).
[24]K.N. Joshipura and P.M. Patel, "Electron Impact Total (Elastic+Inelastic) Cross-Sections of C, N, and O Atoms and their Simple Molecules," Zeitschrift fur Physik D **29**, 269-273 (1994).
[25]L.S. Frost and A.V. Phelps, "Rotational Excitation and Momentum Transfer Cross-Sections for Electrons in H_2 and N_2 from Transport Coefficients," Physical Review **127** (5), 1621 (1962).
[26]M. Blaha and J. Davis, "Elastic Scattering of Electrons by Oxygen and Nitrogen at Intermediate Energies," Physical Review A **12** (6), 2319-2324 (1975).
[27]J.F. Williams and L.J. Allen, "Low-Energy Elastic Scattering of Electrons from Atomic Oxygen," Journal of Physics B **22**, 3529-3539 (1989).
[28]R.L. Taylor and G. Caledonia, "Experimental Determination of the Cross-Sections for Neutral Bremsstrahlung. I. Ne, Ar, and Xe.," JQSRT **9**, 657-679 (1969).
[29]R.L. Taylor and G. Caledonia, "Experimental Determination of the Cross-Sections for Neutral Bremsstrahlung. II. High Temperature Air Species-O, N, and N_2," JQSRT **9**, 681-696 (1969).
[30]R.T.V. Kung and C.H. Chang, "Neutral Bremsstrahlung Radiation," JQSRT **16**, 579-586 (1976).
[31]J.C. Morris, R.U. Krey, and R.L. Garrison, "Bremsstrahlung and Recombination Radiation of Neutral and Ionized Nitrogen," Physical Review **180** (1), 167-183 (1969).
[32]C. Park, Report No. NASA-TM86707, 1985.
[33]E.E. Whiting, C. Park, Liu, Y., Arnold, J.O., and Paterson, J.A., "NEQAIR96, Nonequilibrium and Equilibrium Radiative Transport and Spectra Program: User's Manual.," (1996).
[34]D.H. Menzel and C.L. Pekeris, "Absorption Coefficients and Hydrogen Line Intensities," Monthly Notices of the Royal Astronomical Society **96**, 77-111 (1935).
[35]L. Nedelsky, "Radiation from Slow Electrons," Physical Review **42**, 641-665 (1932).
[36]V.A. Astapenko, V.M. Buimistrov, and Y.A. Krotov, "Bremsstrahlung Accompanied by Excitation and Ionization of the Scattering Atoms," Sov. Phys. JETP **66** (3), 464-471 (1987).

[37]J.C. Keck, R.A. Allen, and R.L. Taylor, "Electronic Transition Moments for Air Molecules," JQSRT **3**, 335-353 (1963).
[38]G.M. Thomas and W.A. Menard, "Measurements of the Continuum and Atomic Line Radiation from High Temperature Air," presented at the 5th AIAA Aerospace Sciences Meeting, New York, NY, 1967 (unpublished).
[39]R.M. Nerem and G.H. Stickford, "Shock-Tube Studies of Equilibrium Air Radiation," AIAA Journal **3** (6), 1011-1018 (1965).
[40]C.O. Laux, R.J. Gessman, and C.H. Kruger, "Modeling the UV and VUV Radiative Emission of High-Temperature Air," 28th AIAA Thermophysics Conference **AIAA 93-2802** (AIAA 93-2802) (1993).
[41]R. Goody and Y. Young, *Atmospheric Radiation*, 2nd ed. (Oxford, 1989).
[42]A Soufiani and J Taine, "High Temperature Gas Radiative Property Parameters of Statistical Narrow-band Models for H_2O, CO_2, and CO and correlated-k Model for H_2O and CO_2," Int. Journal of Heat and Mass Transfer **40**, 987-991 (1997).
[43]L. Pierrot, "Developpement, Etude Critique et validation de modeles de proprietes radiatives infrarouges de CO_2 et H_2O a haute temperature. Application au calcul des transferts dans des chambres aeronautiques et a la teledetection," , Ecole Centrale Paris, 1997.